

STABILITY OF FLIGHT VEHICLE ELASTIC VIBRATIONS WITH CONTROL SYSTEM

Vsevolod I. Smyslov Artyom V. Bykov** and Aleksander P. Pedora****

** Aeroelasticity Department, TsAGI*

Zhukovsky str. 80, Zhukovsky, Moscow Region, Russia, 140180

e-mail: smysl@mail.ru

*** Ground Tests Department, Design Bureau Vimpel JSC*

Volokolamskoye sh. 90, Moscow, Russia, 125424

e-mail: a.bykov@list.ru

**** Aeroelasticity Department, TsAGI*

Zhukovsky str. 80, Zhukovsky, Moscow Region, Russia, 140180

e-mail: a.p.pedora@gmail.com

ABSTRACT

Stability boundaries evaluation for the flight vehicle (FV) elastic oscillations in flight is considered. By example that allows dynamic scheme description of relatively small dimension, the possibility of sufficiently evident and relatively simple technique to consider elements of computational and experimental analysis is demonstrated.

Problems and ways to prevent dangerous elastic vibrations of FV in flight, first of all flutter problem and vibration in a contour including "elastic FV and control system (CS) are examined.

1. Introduction

The present work concerns one of important applied problems of dynamic aeroelasticity: a study of flutter and vibration of system "elastic FV-CS", [1-4]. The main objective is ensuring the flutter safety and aeroelastic stability of oscillations at FV-CS aeroelastic interaction in flight.

In most of these computational and experimental studies frequency methods are used with "frozen coefficients", the variant of contour FV-CS with analogue signals of angular velocity is thus considered. The latter is often acceptable even in the case of digital computer in the path of CS. Further refers to small oscillations only – increments of forces and coordinates; control surfaces are abbreviated as CR (control rudder), control system transducers – CST, rudder rotation axis – RA and rudder drive – RD. Following the traditional division of the basic dynamic aeroelasticity directions into problems of flutter (without CS) and the stability problem of the "elastic FV-CS" contour, further they also are divided. For descriptive reasons the simple examples of vibrations in single plane are considered.

2. Flutter problem

Solution to the flutter problem requires a large amount of computation and experimental works. Preliminary calculations carried out on the simplified model by basis of design documentation basis (it is a subject of discussion). Damping characteristics on the basis of experimental estimates for the FV prototype may be used.

The later executive calculation is based mainly on data obtained from FV GVT [1] with operating RD. In this case, the initial data are: natural frequencies, mode shapes, decrements and general masses of the partial systems, in particular, FV body, CS, and the aerodynamic coefficients. Experimental data is used in the assumption of their greater reliability.

Tests of elastically suspended FV is carried out using a multichannel hardware and software system, including electrodynamic exciters, piezoelectric transducers and data acquisition system, performing the functions of excitation control, measurement, visualization, processing and recording of experimental results [5].

One of the major options for flutter calculating further illustrated by the example of FV, whose natural frequencies of CR flexural and torsional deformations is significantly higher frequencies of the 1st and 2nd bending body mode. Console and body shape model with 4 vibration DOF are analyzed by the prescribed forms method. Vibrations in single plane include: the rotation and "flapping" of rigid CR (figure 1) with a straight rotation axis (flapping is assumed as rotation around an axis parallel to the board chord), and two first FV bending body modes.

As a rule, the estimated case is the maximum dynamic pressure (supersonic), although subsonic flow conditions are considered also. Damping characteristics are presented as linear model by the equivalent viscous friction. The equation of oscillations in the flow for a system with lumped parameters is formulated in traditional form:

$$\mathbf{M}\ddot{\mathbf{q}} + (\mathbf{H} + \mathbf{D}\rho v)\dot{\mathbf{q}} + (\mathbf{K} + \mathbf{B}\rho v^2)\mathbf{q} = 0 \quad (1)$$

where v – flow velocity, ρ – air density, \mathbf{M} , \mathbf{H} , \mathbf{D} , \mathbf{K} , \mathbf{B} – matrices, accordingly, inertia, constructional and aerodynamic damping and stiffness, \mathbf{q} – vector of the generalised coordinates (or degrees-of-freedom). In the case under consideration the elements of matrices \mathbf{M} , \mathbf{H} , \mathbf{K} (symmetric) and a vector \mathbf{q} are:

$$\begin{aligned} m_{11} &= I_{XX}; \quad m_{12} = -I_{XZ}; \\ m_{13} &= S_X \varphi_3 + I_{XZ} \varphi_3'; \quad m_{14} = S_X \varphi_4 + I_{XZ} \varphi_4'; \quad m_{22} = I_{ZZ}; \\ m_{23} &= -S_Z \varphi_3 - I_{ZZ} \varphi_3'; \quad m_{24} = -S_Z \varphi_4 - I_{ZZ} \varphi_4' (x_0); \quad m_{33} = \int m(x) \varphi_3^2(x) dx + I_{ZZ} (\varphi_3')^2 + m_P \varphi_3^2 + 2S_Z \varphi_3 \varphi_3'; \\ m_{34} &= S_Z (\varphi_3' \varphi_4 + \varphi_4' \varphi_3) + I_Z \varphi_3' \varphi_4' + m_P \varphi_3 \varphi_4; \quad m_{44} = \int m(x) \varphi_4^2(x) dx + I_{ZZ} (\varphi_4')^2 + m_P \varphi_4^2 + 2S_Z \varphi_4 \varphi_4'; \\ k_n &= m_{nn} \omega_n^2; \quad h_n = \theta_n k_n / \omega_n \pi; \quad \mathbf{q} = (q_1, q_2, q_3, q_4)^T, \end{aligned}$$

where ω_n , θ_n – partial frequencies and oscillation logarithmic decrements, I_{XX} , I_{XZ} , I_{ZZ} – CR moments of inertia, S_X , S_Z – static moments about the axes OX, OZ, the indices 1 and 2 are corresponding to CR bending and rotation, 3 and 4 – to body 1-st and 2-nd bending modes (φ_3 and φ_4 are values of corresponding body bending mode shapes at RA section), m – distributed body mass, m_R – mass of the rudder. Bending modes are normalized to identity of the x derivative at the RA section: $\varphi_3' = \varphi_4' = 1$. In the case of using natural frequencies and partial mode shapes, the matrix of inertia coefficients \mathbf{M} is full, stiffness and structural damping matrices (\mathbf{K} and \mathbf{H}) are diagonal. The experimental value I_{ZZ} is determined by reduced moment of inertia at the point of rotational vibrations CR excitation, measured at operated RD.

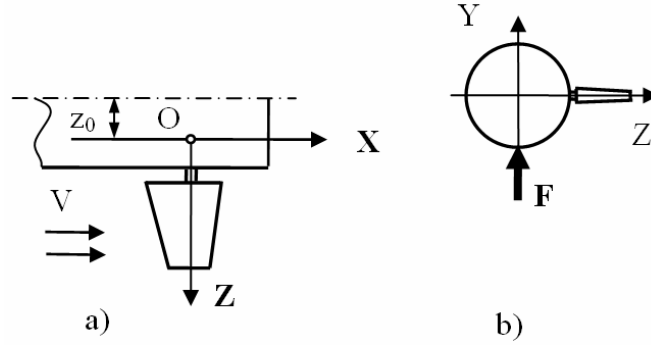


Figure 1: Coordinate system

The structure of \mathbf{D} and \mathbf{B} matrices elements and their dependence on the Mach number are determined by the chosen aerodynamic theory. Unlike more difficult calculations [4] the quasi-steady aerodynamic theory with experimental values of factors $C_Y^\alpha(M)$, $\partial C_m(M)/\partial C_Y(M)$, defined by results of "static" tests in a wind tunnel is used.

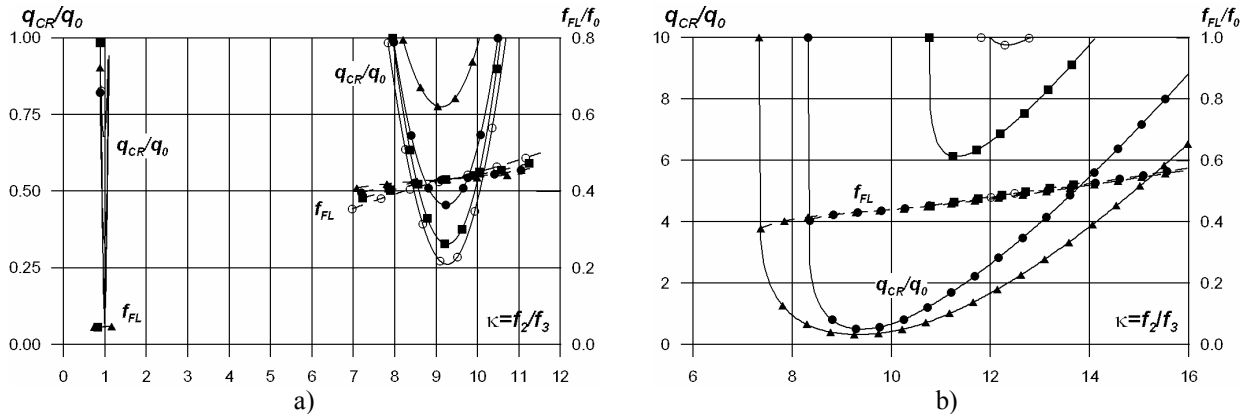


Figure 2: Dependence of q_{KP} and flutter frequencies on CR rotation frequency:

- a) Influence of vibrations decrement of rotation, δ_2 : \circ – 0.10, \blacksquare – 0.25, \bullet – 0.50, \blacktriangle – 1.0;
b) Influence of the relative product of inertia, I_{XZ}/I_{XZ0} : \circ – -0.10, \blacksquare – 0.0, \bullet – 0.50, \blacktriangle – 1.0.

The most significant influence on the result is produced by few parameters only, such as the ratio of the partial frequencies of CR bending and rotation, CR product of inertia, Mach and the oscillation decrements. The results of

calculations are represented mostly as families of dependencies of critical dynamic pressure or the critical flutter velocity vs parameters.

As an example, plots of figure 2 illustrate the calculation results of the relative critical dynamic pressure q_{CR}/q_0 and relative flutter frequency f_{FL}/f_0 , depending on the ratio of CR rotation frequency f_2 to body 1-st mode bending frequency f_3 . Here q_0 and f_0 are constants. Curves on figure 2a correspond to different values of CR rotational vibrations decrement, on figure 2b – to different values of the relative product of inertia (I_{XZ}/I_{XZ0}). The increasing of decrement essentially leads to increasing q_{FL} , also, as increasing of I_{XZ} positive value.

3. Stability of system "elastic FV-CS"

The purpose of this research is defining the possible self-oscillations boundaries and estimation of their level and development means to prevent them with necessary stability margin, if necessary. The general scheme of interaction of elastic FV and CS at vibrations in flight is represented sometimes by three blocks. Considered computational-experimental problem (with the solution *in frequency* domain) requires *experimental* definition of frequency characteristics of separate links. It is possible to explain relationship between transfer functions by the block diagram shown on figure 3. Here three blocks are noted with dot-dash line, and matrix transfer functions connect:

- forces and the moments ("on input"), applied to FV body, with its coordinates ("on output"), \mathbf{W}^{BT} , \mathbf{W}^{BR} and \mathbf{W}^I ;
 - the coordinates of FV body CST section ("on input") with coordinates of body RA, outputs of CS: \mathbf{W}^C , \mathbf{W}^D ;
 - aerodynamic forces and the moments ("on input") with coordinates of wings and CR ("on output"), \mathbf{W}^A .
- The additional forces of "external" excitation applied to FV at GVT, are noted on figure 3 by doubled line.

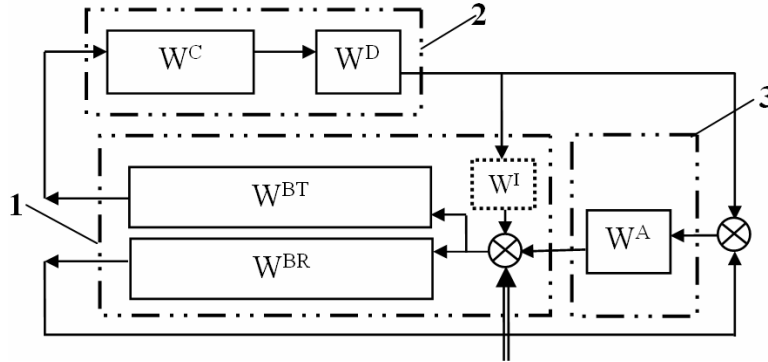


Figure 3: FV transfer functions in flight,
1 – elastic FV, \mathbf{W}^B ; 2 – CS; 3 – aerodynamics.

In the given variant, with reference to the special features of experiment, CR transfer function on figure 3 considers also a control links, that is the dynamic compliance of the chain (gears, backlashes) between shaft of electric motor and CR rotation axis. \mathbf{W}^A remains as a computational component.

The lower loop (blocks 1 and 3) concerns to a flutter problem – with opened chain \mathbf{W}^C . The upper contour includes a problem about self-oscillations elastic FV with included CS with "zero flow" – with opened chain \mathbf{W}^A . Critical flutter velocity is defined (on corresponding frequency), in general, by the relationship:

$$(\mathbf{W}^{BR} \cdot \mathbf{W}^A) = \mathbf{E}, \quad (2)$$

where \mathbf{E} – an unity matrix, the left part is the real value. Almost sufficient condition – equality to unit of one left part elements, on any frequency, believing, for example, vibrations occurring in one plane.

By consideration of lateral oscillations it is possible to present inputs CS vectors by angular speed, ω , and linear acceleration, \mathbf{y} in the CST section, and the outputs of the CS calculator together with correcting filters – by vector control voltages δ_i . The latter are the inputs of the RD. In turn, the outputs of the RD, including control links (they are CS outputs) presented by vector of RD angular output coordinates δ_o .

The "input" of the aerodynamic unit is the sum of the local body angle of attack α_o at RA section (translational coordinate as a whole with the body in the RA section) and the angle δ_o (relative coordinate, the angle relative to the body). They are converted by the airflow in the aerodynamic forces (f_a), and moments (m_a), as a functions of absolute coordinates and their time derivatives. Corresponding vectors can be represented as:

$$\begin{aligned} \omega &= (\omega_Z, \omega_Y)^T; \quad a = (\mathbf{y}_{CST}, \mathbf{z}_{CST})^T; \quad \delta_3 = (\delta_{IZ}, \delta_{IY})^T; \quad \delta_o = (\delta_{OZ}, \delta_{OY})^T; \quad \alpha_o = (\alpha_{OZ}, \alpha_{OY})^T; \\ \mathbf{f}_a &= (f_{AY}, f_{AZ})^T; \quad \mathbf{f}_I = (f_{IY}, f_{IZ})^T; \quad \mathbf{m}_a = (m_{az}, m_{ay})^T; \quad \mathbf{m}_I = (m_{IZ}, m_I)^T, \end{aligned}$$

where f_I , m_I – inertial forces and moments. The additional link of elastic body construction with δ_o allocated dotted line in Figure 3, \mathbf{W}^I , the additional combined excitation of the body – by the force and torque - at oscillations CR outside the airflow. It follows from this possibly, in principle, the difference between the experimental RD frequency

curves, measured on the elastically suspended FV from the corresponding characteristics obtained for the fixed drive compartment. In fact, this inertia link \mathbf{W}^I , realizes by most elastic mass construction and can be generally attributed to the inner link of the FV. Compliance of the RD (the effect on its body vibrational properties of the aerodynamic forces and moments) is not indicate in Figure 3, it appears only when measuring the characteristics of RD on elastically suspended FV and change, in principle, the transfer function \mathbf{W}^I .

In the special case when analyzing, for example, pitch oscillations and taking into account aerodynamic effects only at the RD, the matrix transfer functions are related most simply to the increments of forces and coordinates:

$$\begin{aligned} (\omega_z, \dot{y}_{CST}) &= \mathbf{W}^{BT}(f_y, m_z)^T; \quad (\alpha_0) = \mathbf{W}^{BR}(f_y, m_z)^T; \quad \delta_{3Z} = \mathbf{W}^B(\omega_z, \dot{y}_{CST})^T; \quad \delta_{oz} = \mathbf{W}^H \delta_{IZ}; \\ (f_{AY}, m_{AZ}) &= \mathbf{W}^A(\delta_{oz} + \alpha_{oz}); \quad (f_{IY}, m_{IZ}) = \mathbf{W}^I \delta_{oz}; \quad f_Y = f_{AY} + f_{IY}; \quad m_Z = m_{AZ} + m_{IZ}; \end{aligned} \quad (3)$$

Transfer functions of nonlinear element RD measured for the first harmonic of signal δ_o [6, 7] (with the rupture of \mathbf{W}^C and \mathbf{W}^D) in the presence of an inertial load of RD, i.e., with installed CR. The difference between δ_o angle (it is measured by the signals of feedback potentiometer, FP), and CR absolute angles – $(\delta_o + \alpha)$ are determined by accelerometers, installed on the CR. Figure 4 shows experimental drive frequency response (FR), measured by the FP signals (dotted line shows the absolute angles, measured by accelerometers).

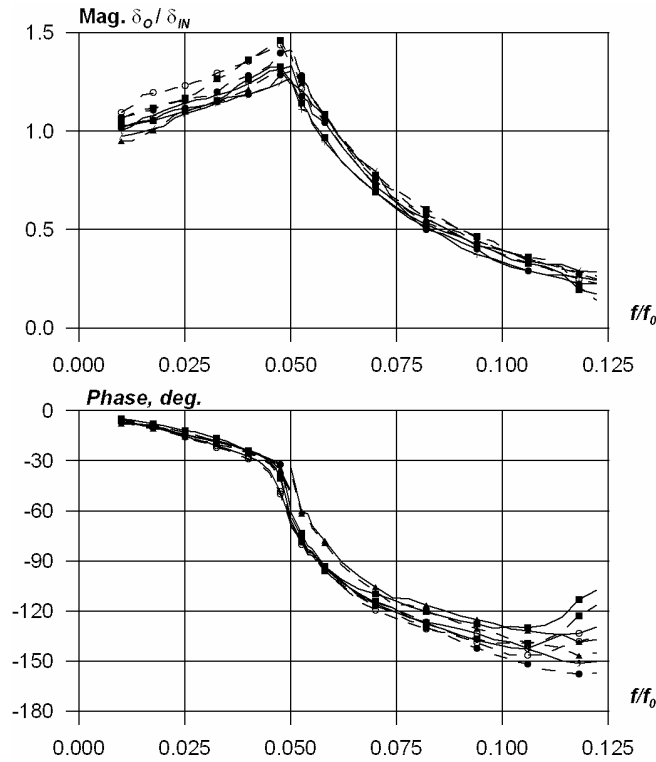


Figure 4. Experimental FR of drive (channels №1-4):

○ – №1, ■ – №2, ● – №3, ▲ – №4

The level of RD input signals (δ_i) for these measurements is selected by the largest magnitude value of \mathbf{W}^D – the ratio δ_o/δ_i . It is determined by the family of amplitude characteristics $\delta_o = f(\delta_i)$, measured at two or three fixed frequencies (in the frequency of elastic body vibrations). While measuring FR of RD at elastically suspended FV, the angles δ_o are recorded also with coordinates of the CST, for example, \dot{y}_{CST} and ω_z .

The transfer functions \mathbf{W}^D for the calculation are formed by the envelopes all measured FR, because of the relatively large scatter of the RD experimental FR, Transfer functions \mathbf{W}^{BR} , \mathbf{W}^{BT} , \mathbf{W}^C at frequencies of body bending vibrations are measured on the body - in the sections CST, RA, as well as on the outputs of CST, at the excitation of oscillations by forces $(F_1 + F_2)$, attached near CR axis (or to the body, in section RA, figure 5). The transfer functions $\mathbf{W}^{BT}_{11} = \omega_z / (F_1 + F_2)$, elements \mathbf{W}^{BR} , $\mathbf{W}^{BT}_{21} = \dot{y}_{CST} / (F_1 + F_2)$, $\mathbf{W}^{BR} = \alpha_{oz} / (F_1 + F_2)$ determined at the same time. FRs of units \mathbf{W}^D , \mathbf{W}^I are determined separately.

In the general case of lateral oscillations the transfer function of the total open loop, \mathbf{W}^U on the angular velocity chain (by opening the inputs RD), is defined as the product:

$$\mathbf{W}^U = \mathbf{W}^0 \cdot (\mathbf{W}^A + \mathbf{W}^I);$$

$$\mathbf{W}^0 = \mathbf{W}^{BT} \cdot \mathbf{W}^C \cdot \mathbf{W}^D,$$

here $(\mathbf{W}^0 \cdot \mathbf{W}^I)$ - transfer function without the flow. Ratio for the full open loop \mathbf{W}^U (the chain ω) is replaced by \mathbf{W} at the closure of an additional circuit α_0 :

$$\mathbf{W} = \mathbf{W}^U \cdot (\mathbf{E} - \mathbf{W}^F)^{-1};$$

$$\mathbf{W}^F = \mathbf{W}^A \cdot \mathbf{W}^{BR},$$

\mathbf{W}^F can be named as "the transfer function of flutter". It characterizes the stability of the lower loop of α_0 , in the flow (figure 3) with an open upper loop, i.e., without CS. Transfer functions of \mathbf{W} and \mathbf{W}^U differs a little at sufficiently high value of the critical flutter speed, otherwise neglecting of \mathbf{W}^F characteristic is unacceptable. Fulfilling of the relation (2) for any frequency means instability for any form of \mathbf{W}^U . Characteristics of \mathbf{W}^A is determined using experimental aerodynamic coefficients, $C_Y^\alpha(M)$, $\partial C_m(M)/\partial C_Y(M)$. In order to avoid the CR deflection, due to the presence of an integrating unit in the chain of linear acceleration, it is replaced by component with the unit ratio.

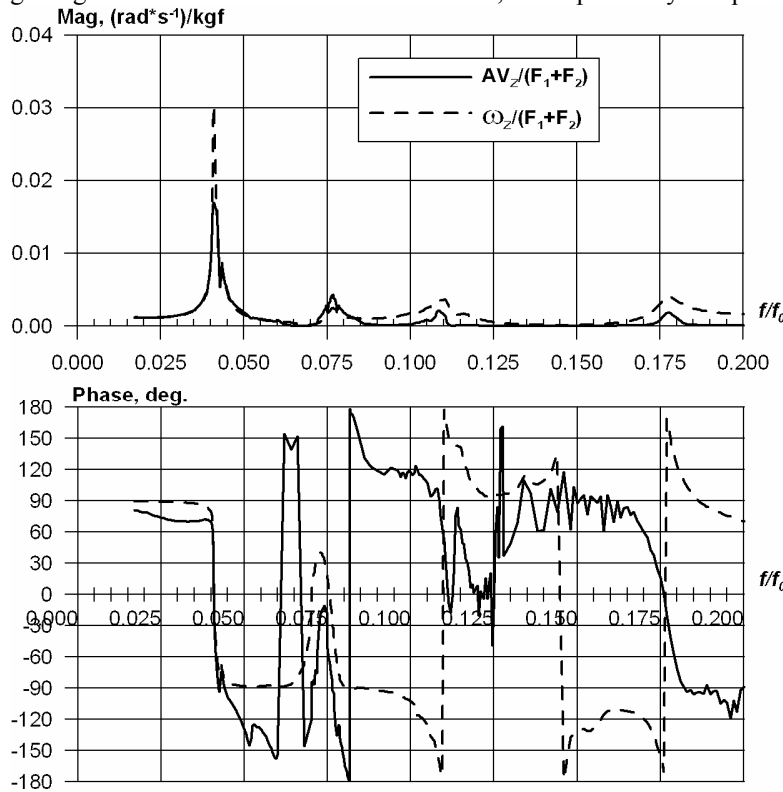


Figure 5. Angular velocity of body (ω_z) and transducer signal of angular velocity (AV_z).

Permissibility of the use of harmonic linearization is based on the properties of the FV body elastic-mass characteristics that filters the higher harmonics.

It has a dependency of the body FR beyond the oscillation amplitude - due to its nonlinear characteristics of stiffness, damping and presence of its "internal" resonances (associated with the CST, etc.). This causes the need for repeated measurements, with different oscillation amplitude. Figure 6 gives an example full open-loop FR in the chain of the angular velocity, \mathbf{W}^U . Figure 6b shows the corresponding frequency hodograph (the numbers marked frequency). For this option, you can note the insufficient value of the stability margins - in particular, less than 2 in absolute value. The transfer function of open loop circuit linear acceleration is defined by similar relations, and the maximum of its modulus in the elastic vibration frequency often substantially less than for a chain of angular velocity. Basic data related to the options test FV with the highest and lowest weight. Data relating to the intermediate solutions generated design mathematical model. This model must be consistent with the experimental - "boundary" versions of the FV.

Primary means of ensuring an necessary stability margins of the contour FV-CS is the corresponding tuning of the corrective filters parameters [5,7]. A method as displacement the CST along the body length, is practically inaccessible in view of the FV design features.

The preliminary estimations of the flow conditions most significant for the stability loss, are located close to the maximum values of the product $(q \cdot K \cdot C_Y^\alpha)$, where K is the coefficient of \mathbf{W}^U . Computing of boundaries and stability margins is carried out using the experimental transfer functions of separate units through calculations FR full open circuit and frequency stability criteria [5-7]. The elements of computational units \mathbf{W}^A are determined by the selected aerodynamic theory.

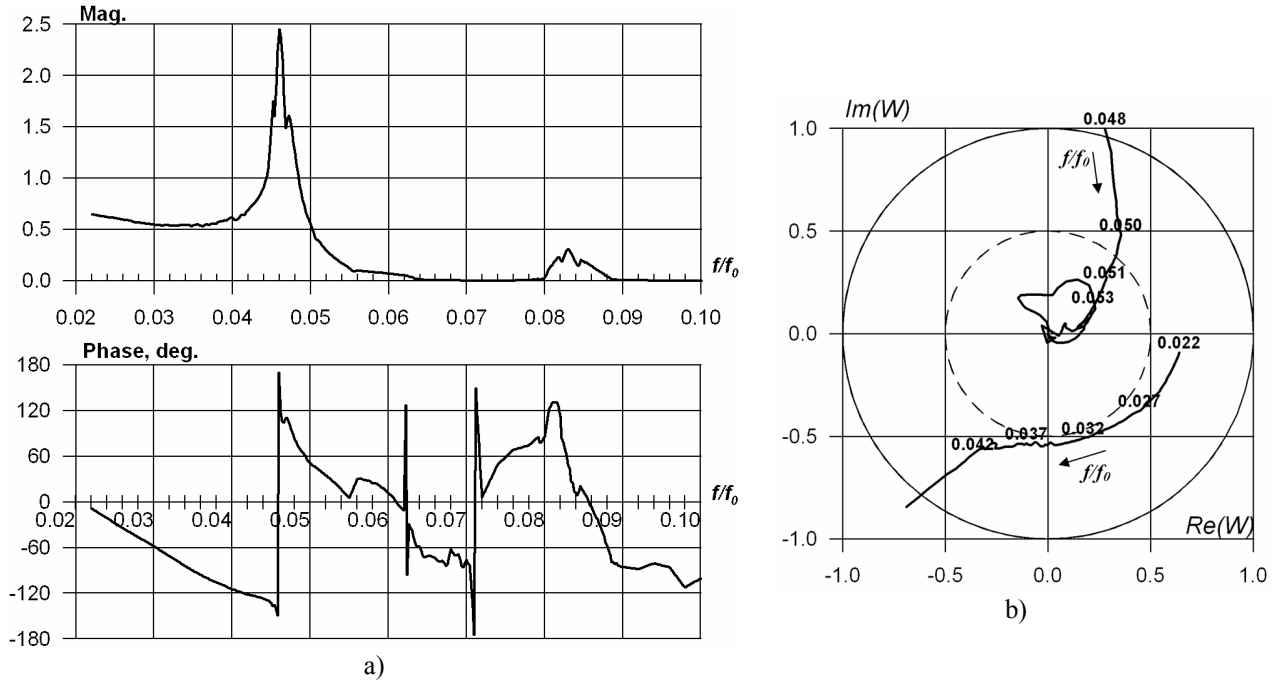


Figure 6. Characteristics of the full open loop: a) FR; b) frequency hodograph.

4. Researches by EMM

The additional means of experiment is the electromechanical simulation of aerodynamic forces, EMM [1,8]. By measurements with the artificial “airflow” they can implement the both tasks, flutter and interaction of elastic FV and CS. Furthermore the experiment with two open loops (and a special case, $v=0$) is added, therefore the studies based on EMM, which relate down these three cases, can be considered as complex. In the case of CS open loop during the aerodynamic forces simulating transfer function \mathbf{W}^F (figure3) is realized, this relates down the flutter problem, when RD are powered on, and the signals $\delta_I = \delta_O = 0$. In the case of EMM with the CS closed loop additionally transfer functions \mathbf{W}^C , \mathbf{W}^D are realized and the signals $\delta_I \neq 0$ and $\delta_O \neq 0$. Amplitude of oscillations in the CST cross-section, caused by the inertial forces (with the presence of relative acceleration $\ddot{\delta}_0$), which correspond to component \mathbf{W}^I , constitutes to 10-15% of total magnitude, measured with forced oscillations with the open loops. This relates to the measurements in the region of the maximum values of \mathbf{W}^{BT} magnitude. In this case the value of the components α_0 is practically incidental.

Experimental scheme is illustrated in figure 7, it is consistent with the block diagram Figure 3. \mathbf{W}^F includes links consisting of transducers, computing devices and exciters with power amplifiers. For clarity, studies of oscillations in the vertical plane with simulating CR forces are shown. Transducers signal processing is realized by specialized computing devices. More details relating to tests with EMM are considered in [1,8]. The matrix of transfer coefficients computing device, K_{CD} , which depend on the calibration of vibration transducers and energizer to amplifiers (matrix, respectively, \mathbf{L} and \mathbf{R}):

$$\mathbf{K}_{CD} = \mathbf{L}^{-1} (v^2 \mathbf{B} + v \mathbf{D}) \mathbf{R}^{-1},$$

where \mathbf{B} , \mathbf{D} - matrices of aerodynamic coefficients. Transfer functions \mathbf{W} and \mathbf{W}^F are realized correctly when measuring the steady-state oscillations with EMM.

Known advantage of the EMM is the possibility of flow conditions simulating on full-scale FV with a functioning CS. In this case, there are no strict limitations on the flow conditions that exist testing, or on duration and amount of tests. The main limitation of the method - effect on the results of selecting the appropriate aerodynamic theory (this restriction pertains to the calculations).

Practically experiments enabled CS is always limited by time. Therefore, these tests are carried out (as well as testing models in a wind tunnel) several numbers of parameters ρ , V , M variants, selected by preliminary calculations. In studies of full-scale FV with the EMM no possibility of varying the bending and rotation CR frequency, one of the main parameters in studies of flutter.

At the same time results obtained by EMM, related to the steady oscillation or transients, with a closed or open loop CS, is a control that take into account both nonlinear elastic structure and elements of the CS, based on dynamic compliance RD (under the influence of inertial and aerodynamic forces). In this case occurs, for example, direct comparison of stability boundaries, obtained by FR calculation open loop (using the experimental FR individual units) and directly measured in a CS closed loop. In this variant can be used in the calculation of the same characteristics of real RD, instead of averaging characteristics, comprised for the stability calculation. The definition of stability margins in the closed loop realizes for this case by a change ratio factor of the unit, introduced additionally.

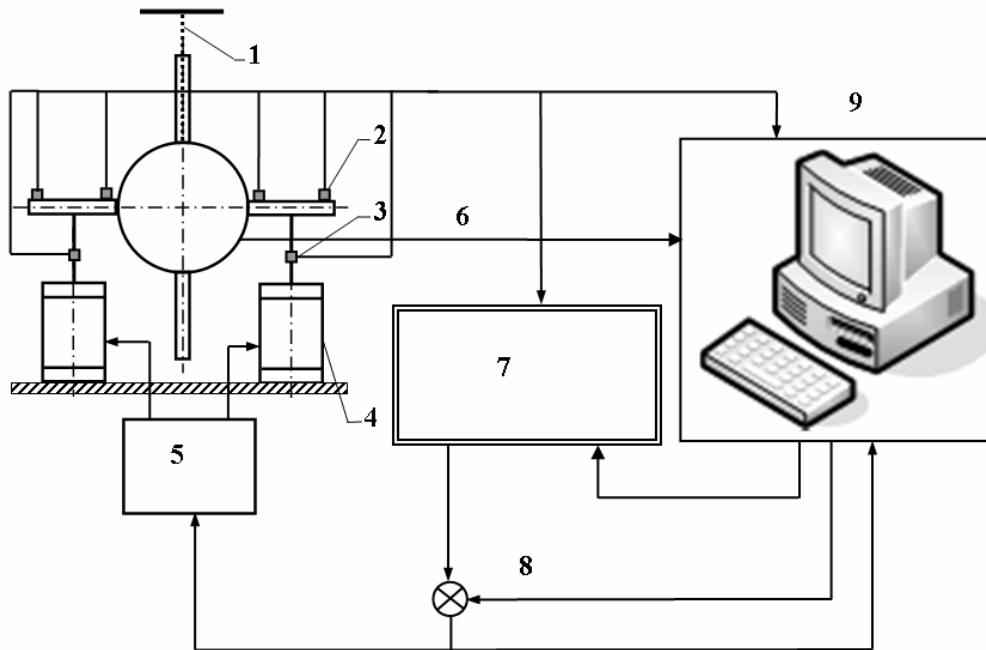


Figure 7. Aerodynamic forces simulation (EMM): 1 – elastic suspension, 2 – accelerometers, 3 – force transducers, 4 – exciters, 5 – power amplifiers, 6 – CS check signals, 7 – special computation device, 8 – external excitation signals, 9 – control facility.

5. Conclusions

On the example that allows dynamic scheme description of relatively small dimension, it is possible the sufficiently evident and relatively simple technique to consider elements of computational and experimental stability boundaries evaluation for the FV elastic oscillations in flight.

The authors express appreciation to A.N. Borodulin, V.N. Volkov and S.G. Parafes for help before the work.

References

- [1] Aeroelasticity. In.: Mechanical Engineering. Enciclopedia. 2002. V. IV-21,
- [2] Kolesnikov K.S., Suhov V. N. 1974. The elastic flight vehicles as object of automatic control. – M: Mechanical engineering.
- [3] Kolesnikov K.S., Minaev A.F. Oscillations of flight vehicles: Vibrations in the technician. 1980. Vol. 3. – M: Mechanical engineering.
- [4] N.I. Baranov, P.D. Nushtaev, Y.P. Nushtaev. 2006. Control Surface Flutter of Aircraft and Rockets. Rusavia, Moscow.
- [5] Bykov A.V., Parafes S.G., Smyslov V.I. 2009. The hardware-software complex for carrying out calculation-experimental researches aeroelastic stability of flight vehicles. *Bulletin MAI*. Vol.16, №5.
- [6] Dovbishchuk V. I, Zichenkov M. Ch, Popovsky V.N. 1996. Application of complex experimental and settlement researches for the decision of problems aeroservoelasticity by working out and plane certification. *Aviation Science and Technology*. № 5-6.

- [7] Pedora A.P., Smyslov V.I. 2005. Research of aeroelastic stability of maneuverable pilotless flight vehicles. *Proceedings of TsAGI*. № 2669.
- [8] Narizhnyj A.G., Pedora A.P., Smyslov V.I. 2001. Vibrating tests with simulating of airflow at aeroelasticity researches on dynamically symylar models. *TsAGI Science Journal*. Vol.XXXII, №1-2.